Genetic interactions between the chromosome axis-associated protein Hop1 and homologous recombination determinants in *Schizosaccharomyces pombe*

Simon David Brown, Olga Dorota Jarosinska, and Alexander Lorenz

Institute of Medical Sciences (IMS), University of Aberdeen, Aberdeen AB25 2ZD, United Kingdom

Key words: *Schizosaccharomyces pombe*, meiosis, homologous recombination, chromosome axis, Hop1

Correspondence should be addressed to:

Alexander Lorenz

Institute of Medical Sciences (IMS)

University of Aberdeen

Foresterhill

Aberdeen AB25 2ZD

United Kingdom

Phone: +44 1224 437323

E-mail: a.lorenz@abdn.ac.uk

Alexander Lorenz ORCID 0000-0003-1925-3713

Abstract

Hop1 is a component of the meiosis-specific chromosome axis and belongs to the evolutionarily conserved family of HORMA domain proteins. Hop1 and its orthologs in higher eukaryotes are a major factor in promoting double-strand DNA break formation and inter-homolog recombination. In budding yeast and mammals they are also involved in a meiotic checkpoint kinase cascade monitoring the completion of double-strand DNA break repair. We used the fission yeast, *Schizosaccharomyces pombe*, which lacks a canonical synaptonemal complex to test whether Hop1 has a role beyond supporting the generation of double-strand DNA breaks and facilitating inter-homolog recombination events. We determined how mutants of homologous recombination factors genetically interact with *hop1*, dissected the role(s) of the HORMA domain of Hop1, and characterized a bio-informatically predicted interactor of Hop1, Aho1 (SPAC688.03c). Our observations indicate that in fission yeast, Hop1 does require a full-length HORMA domain to support wild-type levels of meiotic recombination, although this is not necessary for localization to meiotic chromatin. Furthermore, we show that *hop1*Δ only weakly interacts genetically with mutants of homologous recombination factors, and in fission yeast likely has no major role beyond break formation and promoting inter-homolog events. We speculate that after the evolutionary loss of the synaptonemal complex, Hop1 likely has become less important for regulating meiotic progression in fission yeast, and that this led to a concurrent rewiring of genetic pathways modulating meiotic recombination.

Introduction

Chromosomes of diploid organisms are present in two sets, each derived from one of the parents. To reproduce sexually, this genetic material is halved exactly to produce haploid cells that contain only one chromosome set, the gametes. During fertilization, two gametes from different sexes fuse to form a zygote, re-establishing a double chromosome set. A specialized kind of cell division, called meiosis, is employed to halve the genetic material. In meiosis, one round of chromosome duplication is followed by two rounds of chromosome segregation. Remarkably, correct segregation of chromosomes in meiosis requires formation of double-strand DNA breaks (DSBs) by the conserved transesterase Spo11 (Lam and Keeney 2015), followed by repair through homologous recombination. Homologous recombination, in combination with sister chromatid cohesion, establishes physical connections (chiasmata) between maternal and paternal chromosomes that guide their proper segregation, and promotes reciprocal exchange (crossovers) of maternal and paternal genetic information (Hunter 2015). Careful regulation of this complex process is imperative to ensure the required number of physical links between the correct partner chromosomes, and that unrepaired DNA breaks are mended (Lam and Keeney 2015; Hunter 2015).

The repair of the Spo11-induced DSBs is started by DNA resection. During the initial step of DNA resection Spo11, which is covalently linked to the DNA ends, is endonucleolytically removed by the Mre11-Rad50-Nbs1 (Mre11-Rad50-Xrs2 in *Saccharomyces cerevisiae*) complex in cooperation with Ctp1 (Sae2 in *S. cerevisiae*) (Neale et al. 2005; Hartsuiker et al. 2009). Long-range resection then exposes substantial 3’ tails which are used to invade homologous template DNA on the homologous chromosome or the sister chromatid (strand exchange) to mend the DSB by recombination (reviewed in Mimitou and Symington 2011; Hunter 2015; Lorenz 2017a). Key factors for the strand exchange process in meiosis are the

73 RecA-type recombinases Rad51 and Dmc1 (Shinohara et al. 1997; Grishchuk and Kohli 2003)
74 supported by their mediators Rad55-Rad57, Swi5-Sfr1, and Rlp1-Rdl1-Sws1 (SHU complex in
75 *S. cerevisiae*) (Tsutsui et al. 2001; Grishchuk and Kohli 2003; Akamatsu et al. 2003; Martín et
76 al. 2006; Sasanuma et al. 2013; Hong et al. 2013; Lorenz et al. 2014). These Rad51/Dmc1-
77 mediators are important for generating and stabilizing Rad51/Dmc1 coated nucleoprotein
78 filaments which then invade homologous template DNA (Sung 1997; Haruta et al. 2006). The
79 DNA on the homologous chromosome (or sister chromatid) being invaded is opened as a
80 displacement loop (D-loop) which can then be extended by DNA synthesis using the invading
81 sequence as primer (reviewed in Brown and Bishop 2014). The way, in which D-loops or
82 recombination intermediates derived from it are processed, determines whether repair will
83 occur as a crossover (CO) or a non-CO, and Rad51/Dmc1-mediators play an important role in
84 this (reviewed in Brown and Bishop 2014; Hunter 2015; Lorenz 2017a).
85 In fission yeast processing of most meiotic recombination intermediates into COs and
86 some non-COs depends on the structure-selective endonuclease Mus81-Eme1, the lack of
87 which results in meiotic catastrophe and strongly reduced spore viability (Osman et al. 2003;
88 Smith et al. 2003). Additionally, a sizeable fraction of non-COs is produced by the action of the
89 FANCM-ortholog Fml1, a DEAD/DEAH-box DNA helicase, and it has been shown that Mus81-
90 Eme1 and Fml1 work in parallel to process meiotic recombination intermediates (Lorenz et al.
91 2012). In a wild-type situation Fml1 action seems to be curtailed by Rad51/Dmc1-mediators,
92 because weakening the strand exchange reaction by removing any Rad51/Dmc1-mediator in
93 a *mus81*Δ background ameliorates the strong spore viability defect of *mus81*Δ without
94 restoring CO formation; this rescue depends on the presence of Fml1 (Lorenz et al. 2012,
95 2014).

96 To facilitate the generation of DSBs and their correct repair during meiosis, chromosomes
97 undergo a progression of changes starting with the establishment of meiosis-specific
98 chromosome axes and, in most organisms, culminating in the formation of the synaptonemal
99 complex – an elaborate proteinaceous structure (reviewed in Cahoon and Hawley 2016).
100 Components of the synaptonemal complex seem to be critical for controlling several aspects
101 of meiotic chromosome metabolism, from pairing of homologous chromosomes, to initiation
102 of recombination and maturation of the physical interactions between the homologous
103 chromosomes (reviewed in Cahoon and Hawley 2016; Gray and Cohen 2016). However, some
104 organisms have overcome the necessity for a fully-fledged synaptonemal complex and
105 perform meiosis with a simplified version of it (reviewed in Loidl 2016). The fission yeast
106 *Schizosaccharomyces pombe* is the best-studied organism executing meiosis without a
107 canonical synaptonemal complex (reviewed in Loidl 2006).
108 Despite lacking a synaptonemal complex, fission yeast meiotic chromosomes assemble
109 axes, called linear elements (Olson et al. 1978; Bähler et al. 1993; Molnar 2003), consisting of
110 proteins which are evolutionarily related to axial/lateral elements of the synaptonemal
111 complex (Lorenz et al. 2004). One of these components is Hop1 which, in contrast to other
112 meiotic chromosome axis factors, is conserved on the protein sequence level with homologs
113 from yeast to man (Lorenz et al. 2004; Rosenberg and Corbett 2015). In both *S. cerevisiae* and
114 *Sz. pombe*, Hop1 localizes to the meiosis-specific chromosome axis (Hollingsworth et al. 1990;
115 Smith and Roeder 1997; Lorenz et al. 2004), and deletion of *HOP1/hop1*$^{+}$ causes a decrease in
116 meiotic recombination and homologous chromosome pairing (Hollingsworth and Byers 1989;
117 Loidl et al. 1994; Latypov et al. 2010). Hop1 is characterized by a conserved N-terminal HORMA
118 (Hop1-Rev7-Mad2) domain (Aravind and Koonin 1998) (Fig. 1a) and is the founding member
119 of the meiotic HORMA domain (HORMAD) family proteins. In contrast to yeasts which contain

120 only one meiotic HORMAD (Hop1), higher eukaryotes contain multiple paralogs of meiotic
121 HORMADs: These include HIM-3, HTP-1, HTP-2, and HTP-3 in *C. elegans*; ASY1 and ASY2 in
122 *Arabidopsis*; and HORMAD1 and HORMAD2 in mammals (Zetka et al. 1999; Caryl et al. 2000;
123 Couteau and Zetka 2005; Martinez-Perez and Villeneuve 2005; Goodyer et al. 2008; Fukuda et
124 al. 2010). In fungi, plants, and mammals the HORMA domain is followed by several [S/T]Q
125 residues representing potential Tel1/ATM-Rad3/Mec1/ATR phosphorylation sites, which
126 enable meiotic HORMADs to act as structural adaptors for a meiotic checkpoint kinase cascade
127 (Sanchez-Moran et al. 2007; Carballo et al. 2008; Daniel et al. 2011; Kogo et al. 2012). Fungal
128 Hop1 proteins also contain a centrally located CxxC Zn-finger motif (Hollingsworth et al. 1990)
129 (Fig. 1a) which has been demonstrated to be important for *in vitro* DNA-binding of *S. cerevisiae*
130 Hop1 (Tripathi et al. 2007). Despite its *in vitro* DNA-binding capabilities, Hop1 requires the
131 presence of Rec10 (Red1 in *S. cerevisiae*) to localize to chromosome axes *in vivo* (Smith and
132 Roeder 1997; Lorenz et al. 2004); indeed, Hop1 and Rec10/Red1 have been shown to
133 physically interact with each other (de los Santos and Hollingsworth 1999; Spirek et al. 2010).
134 Rec10 in turn is recruited to chromosome axes by the meiosis-specific cohesin subunit Rec11
135 upon phosphorylation by casein kinase 1 (Phadnis et al. 2015; Sakuno and Watanabe 2015).
136 Here we investigate genetic interactions of *hop1* with meiotic recombination
137 determinants in fission yeast to test whether *hop1* has (a) role(s) beyond its established
138 function in promoting DSB formation (Latypov et al. 2010). Genetic interactions with factors
139 important for recombination intermediate processing (*mus81* and *fml1*) indicated a potential,
140 likely indirect, role for Hop1 in the strand exchange process. However, epistasis analysis with
141 the strand exchange factor *dmc1* and Rad51/Dmc1-mediators (*rad55*, *sfr1,* and *rlp1*) did not
142 support a major separate function of Hop1 in strand exchange. Furthermore, we also show
143 that a full-length HORMA domain is required for wild-type levels of meiotic recombination,

144 but not for localization to meiotic chromatin in *Sz. pombe*. Implications of the evolutionary
145 differences regarding meiotic HORMAD proteins and their interactions are discussed.
146
147 **Material and methods**
148 ***Sz. pombe* and *E. coli* culture conditions**
149 *E. coli* strains were grown on LB and SOC media – where appropriate containing 100 µg/ml
150 Ampicillin (Sambrook and Russell 2000). Competent cells of *E. coli* strains NEB10®-beta (New
151 England BioLabs Inc., Ipswich, MA, USA), and XL1-blue (Agilent Technologies, Santa Clara, CA,
152 USA) were transformed following the protocols provided by the manufacturers.
153 *Sz. pombe* strains used for this study are listed in Table 1. Yeast cells were cultured on
154 yeast extract (YE), yeast nitrogen base glutamate (YNG) and Edinburgh minimal media with
155 glutamate as nitrogen source (EMMG) agar plates containing the required supplements
156 (concentration 250 mg/l on YE, 75 mg/l on YNG and EMMG). Crosses were performed on malt
157 extract (ME) agar containing the required supplements at a final concentration of 50 mg/l,
158 unless strains to be crossed contained plasmids, in which case they were sporulated on
159 sporulation agar with supplements (SPAS) plates with the necessary supplements at 50 mg/l
160 to maintain selection for the plasmids (Smith 2009; Sabatinos and Forsburg 2010).
161 Transformation of yeast strains was done using a standard lithium-acetate procedure (Keeney
162 and Boeke 1994) with the modifications described in Brown and Lorenz (2016).
163 To obtain meiotic *Sz. pombe* cells for chromatin spreading and cDNA preparation
164 meiotic time-courses were executed according to a published protocol (Loidl and Lorenz
165 2009).
166
167 **Yeast strain and plasmid construction**

168 For specifics of strain and plasmid construction please refer to Supplementary Materials.

169 Construction of the *kanMX6*-marked *hop1*Δ*-1* allele has been described previously
170 (Latypov et al. 2010), the *natMX6*-marked *hop1*Δ*-25* was derived from this using an
171 established marker swap protocol (Sato et al. 2005; Lorenz 2015).

172 To produce *hop1*-alleles expressing a particular splice variant, we first partially deleted
173 *hop1* retaining the coding sequence directly upstream of the first and directly downstream of
174 the last intron using a *ura4* marker (Grimm et al. 1988). The resulting strain carrying the *hop1-*
175 *3* allele (UoA725) was subsequently transformed with the cDNA of one of the two splice
176 variants, and candidate strains were selected by resistance to FOA (5-fluoroorotic acid) and
177 then subjected to further testing.

178 Epitope-tagging of Hop1 with 13myc was achieved by cloning a transformation
179 cassette into pFA6a-*13myc-kanMX6* (Bähler et al. 1998) with sequences from the 3' end and
180 downstream flanking region of the *hop1* coding sequence. This transformation cassette was
181 amplified by PCR and transformed into strains UoA746 and UoA868.

182 A deletion cassette for *aho1* was constructed by cloning flanking sequences of
183 *SPAC688.03c* into pAG25 up- and downstream of the *natMX4* marker (Goldstein and
184 McCusker 1999). The resulting plasmid (pALo116) was linearized by a restriction digest and
185 transformed into the standard lab strain FO652.

186 To over-express *aho1*$^{+}$, the coding sequence of *SPAC688.03c* was amplified by PCR and
187 cloned into pREP41-*eGFPC* (Craven et al. 1998).

188 To construct plasmids for over-expression of *hop1*$^{+}$ in *Sz. pombe* we cloned PCR
189 products representing genomic or cDNA versions of the *hop1* coding sequence into pJR-41XL
190 (Moreno et al. 2000). During DNA sequencing we found discrepancies with the *hop1* coding
191 sequence prediction on PomBase (https://www.pombase.org/, last accessed 03/06/2017)

192 (see Results section for details). To corroborate this initial finding we also cloned meiotic cDNA
193 clones from two independently constructed strains (UoA399 and UoA722) into pUC8.
194 All plasmid constructs (for sequences see supporting online material: Lorenz 2017b),
195 as well as epitope-tagged and splice variant strains were verified by DNA sequencing (Source
196 BioScience plc, Nottingham, UK).
197 All DNA modifying enzymes (high-fidelity DNA polymerase Q5, restriction
198 endonucleases, T4 DNA ligase) and NEBuilder HiFi DNA Assembly Master Mix were obtained
199 from New England BioLabs. Oligonucleotides were supplied by Sigma-Aldrich Co. (St. Louis,
200 MO, USA).
201
202 **Genetic and molecular biology techniques**
203 Spot assays to monitor growth and genotoxin sensitivities were essentially performed
204 as described previously (Doe et al. 2000; Lorenz et al. 2009). Spot assays of deletion strains
205 were done on YE plates, and of strains harboring plasmids on EMMG plates containing the
206 required supplements. To repress gene expression from pREP41-type plasmids in strains
207 grown on EMMG, thiamine was added to a final concentration of 4 μM (Sabatinos and
208 Forsburg 2010).
209 Genetic recombination assays and spore viability testing by random spore analysis
210 have been described in detail (Osman et al. 2003; Lorenz et al. 2010, 2012, 2014; Sabatinos
211 and Forsburg 2010).
212 Meiotic cDNA was obtained from cells undergoing synchronized azygotic wild-type
213 meiosis. Aliquots of cell culture were drawn at several time-points during a meiotic time-
214 course by first extracting RNA using the NucleoSpin TriPrep kit (Macherey-Nagel GmbH & Co.
215 KG, Düren, Germany) and then reverse-transcribing the RNA into cDNA using the ProtoScript

216 II First Strand cDNA Synthesis kit (New England BioLabs) following the instructions of the
217 respective manufacturers.
218
219 **Chromatin spreads, immunocytochemistry, and microscopy**
220 Nuclear spreads of meiotic *Sz. pombe* cells were prepared as described previously (Loidl and
221 Lorenz 2009), with the only modification that Lallzyme MMX (Lallemand Inc., Montréal,
222 Canada) at a final concentration of 100 mg/ml was used as the sole enzyme in the
223 spheroplasting solution (Flor-Parra et al. 2014).
224 Immunostaining was performed as previously described (Loidl and Lorenz 2009) using
225 polyclonal rabbit α-myc (ab9106; Abcam PLC, Cambridge, UK) at a 1:500 dilution as the
226 primary antibody. Antibody-bound protein was visualized using donkey α-rabbit IgG
227 AlexaFluor-555 (ab150062; Abcam) at a 1:500 dilution as a secondary antibody conjugated to
228 a fluorophore. DNA was stained by Hoechst 33342 (Molecular Probes, Eugene, OR, USA) at a
229 final concentration of 1 μg/ml.
230 Analysis was done using a Zeiss Axio Imager.M2 (Carl Zeiss AG, Oberkochen, Germany)
231 epifluorescence microscope equipped with the appropriate filter sets to detect red and blue
232 fluorescence. Black-and-white images were taken with a Zeiss AxioCam MRm CCD camera
233 controlled by AxioVision 40 software v4.8.2.0. Images were pseudo-coloured and overlayed
234 using Adobe Photoshop CC (Adobe Systems Inc., San José, CA, USA).
235
236 **Data presentation and statistics**
237 Data presented as box-and-whisker plots were created in RStudio 1.0.136 (R version 3.3.1)
238 (http://www.r-project.org/) using the boxplot() function with its standard settings. The lower
239 and upper 'hinges' of the box represent the first and third quartile, respectively, and the black

240 bar within the box indicates the median (=second quartile). The 'whiskers' represent the
241 minimum and maximum of the range, unless they differ more than 1.5-times the interquartile
242 distance from the median. In the latter case, the borders of the 1.5-times interquartile
243 distance around the median are indicated by the 'whiskers' and values outside this range
244 ('outliers') are shown as open circles. Raw data and R scripts used for the boxplot() function
245 are available online as supporting material (Lorenz 2017b).

246 Initially, all data involving multiple comparisons underwent an overall statistical
247 assessment using a Kruskal-Wallis one-way analysis of variance to verify that there indeed are
248 statistically significant differences ($\alpha < 0.05$) between data sets within one experiment. All
249 direct one-on-one statistical comparisons between control and experimental data were done
250 using a two-tailed Mann-Whitney U test. Both Kruskal-Wallis and Mann-Whitney U tests are
251 non-parametric and therefore do not assume normal distribution of data points within a data
252 set. Kruskal-Wallis analyses were performed in IBM SPSS Statistics 24.0.0.0 (International
253 Business Machines Corporation, Armonk, NY, USA), and Mann-Whitney U tests in G*Power
254 3.1.9.2 (Faul et al. 2007, 2009). *P* values listed in Supplementary Tables S1 and S2 were
255 determined with a statistical power ($1 - \beta$) set to 0.8.

256

257 **Results**

258 **Correction of the *Sz. pombe hop1* coding sequence**

259 When constructing plasmids to over-express *hop1*$^{+}$ in fission yeast cells, sequencing of our
260 cDNA clones revealed major discrepancies compared to the annotated sequence on PomBase
261 (https://www.pombase.org/, last accessed 03/06/2017). These differences resulted from the
262 incorrect annotation of the position of the third intron (Figs. 1b, S1, S2). Additionally, we
263 detected two splice variants (sv) of *hop1* (http://www.ebi.ac.uk/ena/data/view/PRJEB22374).

264 The main cDNA version (*hop1-sv1*) translated into a protein with 527 amino acids (AAs) in
265 length which is one AA shorter than the currently annotated one (528 AAs). The discrepancy
266 affects AAs 138-156/157 in the core region of the HORMA domain (Fig. 1). A second, shorter
267 splice variant (*hop1-sv2*) seems to use a downstream AG as an alternative splice acceptor site,
268 thereby expanding the third intron by another 21 bps (Figs. 1b, S1, S2). In a total of 25 cDNA
269 clones from meiotic cDNA preparations of two independently constructed strains drawn from
270 different time-points of a meiotic time-course, 23 were of the *hop1-sv1* type, one conformed
271 to the *hop1-sv2* type, and one was aberrant representing a rather short form of *hop1* with a
272 frame-shift (Fig. 1c). Considering the scarcity of *hop1-sv2* in our samples it could well represent
273 a splicing accident or even a PCR artefact.

274 Using ClustalΩ (Sievers et al. 2014) the translation of the experimentally determined
275 Hop1-sv1 HORMA domain sequence also produces a slightly better alignments with Hop1
276 HORMA domains of other *Schizosaccharomyces* (Fig. S3) species than the predicted one. The
277 region of discrepancy in the experimentally derived *Sz. pombe* Hop1 HORMA domain
278 (VCKFFNRLHESFIKLINVQKE) aligns without much gapping (only one AA position in *Sz.*
279 *octosporus* and *Sz. cryophilus* shows a gap) and 7 fully conserved or strongly similar positions
280 to its counterpart in the other *Schizosaccharomyces* species. The same region from the
281 predicted *Sz. pombe* Hop1 (VSYQRSERFVIKLFLSGNVKTE) produces a large gap in the alignment
282 with the *Sz. japonicus* sequence, receives a three AAs gap compared to *Sz. octosporus* and *Sz.*
283 *cryophilus*, and aligns with only 4 fully conserved or strongly similar positions. Over the whole
284 length of the HORMA domain in this multi-species comparison, this results in 10 fully
285 conserved and 34 strongly similar AA residues in the alignment for the predicted *Sz. pombe*
286 Hop1 sequence, and in 11 fully conserved and 35 strongly similar AA residues with the
287 experimentally derived one (Fig. S3). This demonstrates that the current annotation of the

288 *hop1* open reading frame on PomBase (https://www.pombase.org/) is erroneous, and that
289 the long, predominant splice variant (*hop1-sv1*) we identified in our cDNA clones is the correct
290 transcript of *hop1*.
291
292 **The long *hop1* splice variant *hop1-sv1* is sufficient for meiotic recombination**
293 We were interested in establishing whether the long, predominant version of Hop1 (Hop1-
294 sv1) is fully functional, and whether solely expressing the rare short version Hop1-sv2 (lacking
295 7 AAs in the HORMA domain, see Fig. 1) causes a phenotype. In *S. cerevisiae* removing the N-
296 terminal 268 AAs of Hop1 – which includes the HORMA domain – has previously been shown
297 to abolish spore viability completely, however the C-terminal fragment remaining is still
298 capable of binding DNA *in vitro* (Khan et al. 2013). In contrast, the *M127K* point mutation in
299 the center of the HORMA domain of *C. elegans HTP-1*, one of four meiotic HORMA-paralogs
300 in the nematode, results in only a minor meiotic phenotype despite HTP-1^{M127K} not localizing
301 to meiotic chromosome axes (Silva et al. 2014). The *Sz. pombe* short form *hop1-sv2* is
302 apparently not strongly expressed (if not a splicing accident or PCR artefact) and thus unlikely
303 to play a (major) role in a wild-type background. However, in light of the distinct phenotypes
304 of HORMA-domain mutants in budding yeast and *C. elegans*, we wanted to use the *hop1-sv2*
305 variant to probe the role of the HORMA domain for meiotic recombination and Hop1
306 localization to meiotic chromatin in fission yeast. The 7 AAs (positions 157-163) missing in
307 Hop1-sv2 are close to the boundary between the HORMA core domain and the HORMA
308 "safety-belt" region (Fig. 1a, b; Fig. S2) (Rosenberg and Corbett 2015), and their loss might
309 affect interaction of Hop1 with the meiotic chromosome axis similar to nematode HTP-1^{M127K}
310 and also interfere with Hop1's self-oligomerization.

311 Previously, it has been shown that the full deletion of *hop1* causes a reduction in both
312 intragenic (gene conversion) and intergenic (crossover) recombination at several genetic
313 intervals in fission yeast with a concomitant increase in intrachromosomal recombination
314 (Latypov et al. 2010). The *hop1* deletion also leads to defects in homologous pairing along
315 chromosome I during meiosis (Latypov et al. 2010). These phenotypes can at least be partially
316 explained by a reduction in DSB formation and a preponderance of DSBs being repaired from
317 the sister chromatid rather than the homolog (Rothenberg et al. 2009; Latypov et al. 2010).
318 Using our meiotic recombination assay system (Lorenz et al. 2010) which allows us to
319 concomitantly measure spore viability, and the frequency of gene conversion (GC), crossovers
320 (COs) and COs with GC events we found a statistically significant decrease in all recombination
321 measures in a *hop1*Δ compared to a wild-type cross (Fig. 2). Indeed, GC decreased 4.7-fold (p
322 $= 4.53 \times 10^{-13}$) (Fig. 2b), COs 2.8-fold ($p = 3.61 \times 10^{-6}$) (Fig. 2c), and COs associated with GC
323 events were reduced by 8.7 percentage points ($p = 0.01$) (Fig. 2d) (see also Table S1). Overall,
324 this reduction in recombination outcome did not negatively affect spore viability (Table S1).
325 Recombination of a strain expressing only the long, predominant version *hop1-sv1* (from the
326 *hop1*-promoter at its original locus without any marker genes inserted) was indistinguishable
327 from wild type, whereas replacing the wild-type copy of *hop1* with *hop1-sv2* led to a moderate
328 reduction in GC (1.4-fold, $p = 1.51 \times 10^{-3}$) and COs (1.7-fold, $p = 2.27 \times 10^{-3}$), but not in COs
329 associated with GC events ($p = 0.76$) compared to wild type (Fig. 2, Table S1). This indicates
330 that in line with *hop1-sv1* being the predominant, if not the exclusive, splice variant it behaves
331 like wild-type *hop1* containing all its introns, whereas *hop1-sv2* is not fully functional and
332 produces a hypomorphic phenotype.
333

334 **Hop1 localizes to meiotic chromatin and forms linear elements independent of a full-length**
335 **HORMA domain**

336 As with organisms possessing a fully-fledged synaptonemal complex, Hop1 localizes to meiotic
337 chromosome axes, called linear elements, in fission yeast (Lorenz et al. 2004). However, the
338 deletion of *hop1* has little impact on linear element formation *per se* (Lorenz et al. 2006). We
339 were keen to understand whether a full-length HORMA domain is required for localization of
340 Hop1 to linear elements. We used immunostaining on chromatin spreads from meiotic fission
341 yeast cells to detect heterozygously 13myc-tagged Hop1-sv1 and Hop-sv2 in homozygous
342 *hop1-sv1* and *hop1-sv2* strains, respectively. Hop1-sv1-13myc formed linear elements, and all
343 four morphological classes of linear elements (dots, threads, networks, and bundles) were
344 observed (Fig. 3a-d) (Bähler et al. 1993; Lorenz et al. 2004, 2006). This result is consistent with
345 the wild-type phenotype for meiotic recombination of *hop1-sv1* crosses. Intriguingly, Hop1-
346 sv2-13myc was indistinguishable from Hop1-sv1-13myc (Fig. 3e-h). Therefore, the loss of the
347 7 AAs close to the boundary between the HORMA core domain and the HORMA "safety-belt"
348 region in the *hop1-sv2* allele does not conspicuously influence recruitment of Hop1 to linear
349 elements, despite affecting meiotic recombination (Fig. 2b-d).

350

351 **Searching for Hop1 interactors**

352 A bio-informatics screen using the *Pombe* Interactome (PInt) (Pancaldi et al. 2012) for
353 potential Hop1 interactors retrieved *SPAC688.03c* as the highest hit from an uncharacterized
354 open reading frame (10th highest overall). The gene product of *SPAC688.03c* localizes
355 preferentially to the nucleus (Matsuyama et al. 2006) (Fig. S4) and is upregulated at the onset
356 of meiosis (Mata et al. 2002), which is consistent with a potential role in meiotic chromatin
357 metabolism. Notably, a point mutation in the human ortholog of *SPAC688.03c*, *AMMECR1*, is

358 associated with Alport syndrome (A), mental retardation (M), midface hypoplasia (M), and
359 elliptocytosis (E) (Vitelli et al. 1999; Andreoletti et al. 2017). Therefore, we investigated the
360 phenotype of a *SPAC688.03c* (from here on *aho1*, for *AMMECR1-homolog*) deletion in
361 vegetative and generative cells.

362 First, *aho1*Δ was assayed for changes in genotoxin sensitivity and meiotic
363 recombination outcome. The wild-type and *aho1*Δ strains exhibited similar levels of resistance
364 to the topoisomerase I-poison camptothecin (CPT), the alkylating agent methyl
365 methanesulfonate (MMS), the ribonucleotide reductase blocker hydroxyurea (HU), and
366 ultraviolet (UV) radiation (Fig. 4a). The deletion of *aho1* in a wild-type or *hop1*Δ background
367 did not affect spore viability (Fig. 4b). The meiotic recombination outcome of an *aho1*Δ single
368 mutant was similar to wild type, and an *aho1*Δ *hop1*Δ double mutant was indistinguishable
369 from a *hop1*Δ single mutant, except for a moderate 1.4-fold reduction in gene conversion (p
370 = 0.034) (Fig. 4c-e, Table S1). These results indicate that under standard laboratory conditions
371 *aho1*$^+$ is not required for DNA damage repair or meiotic recombination. Therefore, Aho1 is not
372 an essential interactor of Hop1 because it does not mirror the phenotype of *hop1*Δ and we
373 did not observe strong genetic interactions with *hop1*Δ.

374 We tested whether over-expression of *aho1*$^+$ might uncover a DNA repair and/or
375 recombination role. The *aho1*$^+$ gene was put under the control of the thiamine-repressible
376 *nmt1*-promoter at the medium pREP41-level and tagged with GFP at its C-terminus. Spot
377 assays and recombination assays were performed after Aho1-GFP over-expression was
378 induced for 24 hours (see also Fig. S4). Cells over-expressing Aho1-GFP did not show increased
379 genotoxin sensitivities compared to cells containing an empty plasmid, cells over-expressing
380 GFP alone, or cells grown in the presence of thiamine (in which expression is not induced) (Fig.
381 5a, b). Over-expression of Aho1-GFP also did not alter spore viability and meiotic

382 recombination outcome in comparison to GFP over-expression (Fig. 5c-f, Table S2), indicating
383 that a massive surplus of Aho1 protein has no negative impact on reproductive success.
384
385 **_hop1_ displays genetic interactions with the structure-selective endonuclease _mus81_ and the**
386 **DNA helicase _fml1_**
387 Considering that the absence of *hop1* reduces recombination outcome in a similar fashion to
388 Rad51/Dmc1-mediator (*rad55-rad57*, *swi5-sfr1*, and *rlp1-rdl1-sws1*) mutants (Lorenz et al.
389 2012, 2014) (Fig. 2) we were wondering how *hop1* genetically interacts with the key meiotic
390 determinants of CO and non-CO formation, *mus81* and *fml1*.
391 The deletion of *hop1*Δ in a *mus81*Δ background improves spore viability from ~1.5%
392 (Lorenz et al. 2010) to 18.7% (Fig. 6, Table S1) similar to what has been seen in *mus81*Δ
393 Rad51/Dmc1-mediator double mutants (Lorenz et al. 2012, 2014). This rescue in spore viability
394 is not accompanied by a restoration of CO frequency. A *hop1*Δ *mus81*Δ mutant shows only
395 0.2% of COs which is significantly different both from wild type ($p = 1.9 \times 10^{-7}$) and the *hop1*Δ
396 single mutant ($p = 2.7 \times 10^{-3}$) (Fig. 6c, Table S1). Also, the rate of COs associated with GC events
397 at 0.71% is significantly lower in the double mutant than in the wild type (63.0%, $p = 5.3 \times 10^{-}$
398 ^{12}) or the *hop1*Δ single mutant (54.3%, $p = 3.4 \times 10^{-15}$) (Fig. 6d, Table S1).
399 Removal of *fml1*$^{+}$ increases COs associated with GC events to 72.2% (~10 percentage
400 points more than wild type) (Lorenz et al. 2012), but has little effect on other recombination
401 outcomes. In *fml1*Δ *hop1*Δ double mutants, there are 72.6% of COs associated with GC events
402 which is significantly different from both wild type ($p = 3.4 \times 10^{-3}$) and a *hop1*Δ single mutant
403 ($p = 4.9 \times 10^{-9}$) (Fig. 6d). Overall CO formation is not changed compared to *hop1*Δ ($p = 0.78$),
404 but significantly different from wild type ($p = 7 \times 10^{-7}$) (Fig. 6c). Also GC frequency is unchanged

405 compared to *hop1*Δ (p = 0.49) (Fig. 6b) suggesting that in the absence of *hop1*$^+$ the DNA
406 helicase Fml1 does not gain any additional functionality.
407
408 ***hop1* does not show strong genetic interactions with Rad51/Dmc1-mediator mutants**
409 Rad51/Dmc1-mediators are highly conserved, positive determinants of meiotic recombination
410 (Schwacha and Kleckner 1997; Ellermeier et al. 2004; Hayase et al. 2004; Bleuyard et al. 2005;
411 Hyppa and Smith 2010; Lorenz et al. 2012, 2014; Sasanuma et al. 2013). In fission yeast the
412 meiotic recombination phenotype of the *hop1*Δ crosses strongly resembles that of
413 Rad51/Dmc1-mediator mutants in that it reduces all meiotic recombination outcomes and
414 alleviates the effects of a *mus81*Δ mutants (see above). Therefore, we were interested in how
415 *hop1* genetically interacts with the mediators *sfr1*, *rad55*, and *rlp1*, as well as *dmc1* itself. The
416 deletion of *hop1*$^+$ leads to a notable reduction in DSB formation (Rothenberg et al. 2009;
417 Latypov et al. 2010), and some of the decrease in recombination frequency in *hop1*Δ is likely
418 due to low DSB formation. This reduction may be unrelated to Rad51/Dmc1-mediator
419 function, because absence of the Sfr1-cofactor *swi5*$^+$ or of *dmc1*$^+$ does not appreciably reduce
420 DSB formation (Young et al. 2004). We pose that in the absence of *hop1*$^+$, which contributes
421 to the establishment of a meiosis-specific chromatin environment, successful sexual
422 reproduction will become more reliant on the mitotic repair factors Rad55 and Rlp1.
423 Therefore, we expected a substantial negative genetic interaction of *hop1* with *sfr1*, *rad55*,
424 *rlp1*, and *dmc1*.
425 Indeed, *hop1*Δ *rad55*Δ and *hop1*Δ *rlp1*Δ double mutants displayed significantly lower
426 GC ($p = 5.3 \times 10^{-5}$ and p = 0.02, respectively) than a *hop1*Δ single mutant (Fig. 7a , Table S1);
427 the GC level is also notably lower than in *rad55*Δ (0.52%) and *rlp1*Δ (0.36%) (Lorenz et al.
428 2014). However, overall CO frequency and COs associated with GC events were not different

429 from *hop1*Δ in *hop1*Δ *rad55*Δ and *hop1*Δ *rlp1*Δ (Fig. 7b, c; Table S1). Deletion of *sfr1*$^{+}$
430 decreased GC rate by 7.5-fold in a *hop1*Δ background to 0.036% ($p = 1.4 \times 10^{-8}$) (Fig. 7d, Table
431 S1) which is also substantially lower than the 0.13% found in an *sfr1*Δ single mutant (Lorenz
432 et al. 2014). Other recombination outcomes were indistinguishable from *hop1*Δ (Fig. 7e, f;
433 Table S1). The interaction of *hop1*Δ with *dmc1*Δ is completely epistatic (Fig. 7d-f, Table S1).
434 Importantly, no noteworthy decreases of spore viability have been observed in any of the
435 double mutants (Table S1). This stands in contrast to double mutant combinations of
436 Rad51/Dmc1-mediators with each other or with *dmc1*Δ; *dmc1*Δ *rad55*Δ, *dmc1*Δ *rlp1*Δ, *rad55*Δ
437 *sfr1*Δ and *rlp1*Δ *sfr1*Δ display strong synergistic reductions in spore viability (Lorenz et al.
438 2014). Overall, this suggests that in fission yeast meiosis the absence of *hop1*$^{+}$ does not
439 generate a situation which necessitates the presence of a fully functional recombination
440 machinery to produce viable progeny.
441
442 **Discussion**
443 Here we characterize the genetic interactions of *hop1*, which encodes a meiotic HORMA
444 domain protein, with homologous recombination factors in fission yeast. Meiotic HORMADs
445 are components of the meiosis-specific chromosome axis which promote DSB formation to
446 allow for the efficient pairing of homologous chromosomes. At the same time HORMADs
447 attenuate undesirable recombination between sister chromatids (reviewed in Rosenberg and
448 Corbett 2015). In organisms possessing a synaptonemal complex, HORMADs support its
449 formation, and depending on the organism may mount a checkpoint arrest when DSB repair
450 is not completed or homologous chromosomes are not synapsed (Woltering et al. 2000;
451 Armstrong et al. 2002; Couteau and Zetka 2005; Martinez-Perez and Villeneuve 2005; Carballo
452 et al. 2008; Daniel et al. 2011; Rinaldi et al. 2017). *Sz. pombe* meiosis progresses without the

453 formation of a synaptonemal complex, therefore any roles related to the synaptonemal
454 complex will likely not apply. Indeed, DSB formation is reduced and inter-sister recombination
455 is increased in fission yeast *hop1*Δ (Rothenberg et al. 2009; Latypov et al. 2010). Consistent
456 with DSB reduction, decreased numbers of Rec7-foci (an essential co-factor of Spo11) have
457 been observed when Hop1 was absent (Lorenz et al. 2006). As a result of DSB reduction,
458 meiotic inter-homolog recombination frequencies are lower in *hop1*Δ than in wild type
459 (Latypov et al. 2010) (Fig. 2). Thus, the Hop1 function in promoting DSB formation seems to
460 be conserved in fission yeast. In budding yeast Hop1 also acts downstream of DSB formation
461 in promoting Dmc1-dependent inter-homolog recombination by preventing Dmc1-
462 independent Rad51-driven recombination (Niu et al. 2005; Carballo et al. 2008). The
463 suppression of inter-sister recombination is achieved by Hop1-dependent activation of Mek1
464 which in turn phosphorylates and deactivates the Rad51-mediator Rad54, and also
465 phosphorylates and activates the meiosis-specific Rad51-inhibitor Hed1 (Tsubouchi and
466 Roeder 2006; Niu et al. 2009; Callender et al. 2016). Together, this regulatory network has
467 specific genetic consequences: (I) meiotic recombination cannot proceed without Dmc1 which
468 causes a meiotic arrest resulting in an inability to sporulate, and (II) deleting *hop1* in a *dmc1*Δ
469 background restores spore formation by allowing Rad51-dependent DSB repair (Niu et al.
470 2005; Carballo et al. 2008). In fission yeast the genetic interaction between *hop1* and *dmc1*
471 looks quite different (Fig. 7) in that it is epistatic, however neither single mutant has as strong
472 a phenotype as the corresponding mutants in *S. cerevisiae* (Hollingsworth and Byers 1989;
473 Bishop et al. 1992; Grishchuk and Kohli 2003; Latypov et al. 2010). Two features may account
474 for this apparent difference between the two yeasts: The budding yeast is probably the only
475 organism which shuts down Rad51 strand exchange activity via Hed1 (Tsubouchi and Roeder
476 2006), and fission yeast employs both Rad51 and Dmc1 in their direct strand exchange

477 capacity (Grishchuk and Kohli 2003). Interestingly, the genetic interaction of meiotic *Hormad*
478 and *dmc1* genes generally does not show much conservation. In *Arabidopsis* mutation of *asy1*
479 or *dmc1* causes a strong reduction or absence of chiasmata, respectively, leading to fertility
480 defects. However, the *asy1 dmc1* double mutant looks like a *dmc1* single mutant (Sanchez-
481 Moran et al. 2007). In the mouse both *Dmc1*$^{-/-}$ and *Hormad1*$^{-/-}$ single mutants undergo meiotic
482 arrest at mid-pachytene, and so does the *Dmc1*$^{-/-}$ *Hormad1*$^{-/-}$ double mutant (Daniel et al.
483 2011), i.e. there is no reciprocal rescue as in *S. cerevisiae hop1*Δ *dmc1*Δ. These disparate
484 observations in various model organisms suggest that the genetic networks controlling DSB
485 repair and CO formation, and how these processes are integrated with chromosome axis
486 organization, have undergone considerable rewiring during evolution. Because fission yeast
487 relies on both Rad51 and Dmc1 to invade a repair template during meiotic DSB repair, we also
488 looked at the genetic interaction of *hop1* with Rad51/Dmc1-mediator mutants. Apart from an
489 additive effect on GC frequency in *hop1*Δ *rad55*Δ, *hop1*Δ *rlp1*Δ, and *hop1*Δ *sfr1*Δ double
490 mutants, which can easily be explained by the early functions of Hop1 (reduced DSB formation
491 and increased inter-sister recombination), other recombination outcomes were not different
492 from the *hop1*Δ single mutant (Fig. 7). This indicates that in a fission yeast *hop1*Δ mutant
493 gamete production does not become more reliant on strand exchange than in a wild-type
494 background.
495 Genetic interaction of *hop1*Δ with *mus81*Δ resembled that of *mus81*Δ combined with mutants
496 affecting strand exchange (Ellermeier et al. 2004; Lorenz et al. 2012, 2014), rescuing *mus81*Δ's
497 spore viability defect without rescuing its CO defect (Fig. 6). Again this interaction can be
498 explained by Hop1 promoting DSB formation and inter-homolog recombination.
499 It is well established that fungal Hop1 localizes to the chromosome axis during meiotic
500 prophase by physically interacting with the linear/lateral element protein Rec10/Red1 in

501 fission and budding yeast, respectively (de los Santos and Hollingsworth 1999; Spirek et al.
502 2010). Considering Hop1's central role in coordinating meiotic progression, it is not unlikely
503 that it would physically interact with previously uncharacterized meiotic players; indeed with
504 IHO1, a novel HORMAD1-interactor has recently been described in mice (Stanzione et al.
505 2016). A bio-informatical protein interaction-predictor PInt (Pancaldi et al. 2012) suggested
506 that the uncharacterized AMMECR1-homolog Aho1 might be a potential Hop1-interactor in
507 fission yeast. However, neither deletion nor over-expression of Aho1 indicates a clear meiotic
508 function, independent of the presence or absence of Hop1 (Figs. 4, 5).
509 One of the determining features of Hop1 is its HORMA domain whose function was enigmatic
510 until recently, when it was implicated in the recruitment of Hop1 to the meiotic chromosome
511 axis and in its self-assembly into larger homomeric complexes (Kim et al. 2014; Rosenberg and
512 Corbett 2015). We exploited a cDNA clone of *hop1* (*hop1-sv2*) which produces a protein that
513 lacks 7 AAs in the HORMA domain to examine whether a full-length HORMA domain in fission
514 yeast Hop1 is essential for its function and localization. Interestingly, expressing Hop1-sv2 in
515 place of wild-type Hop1 did not result in a notable reduction in localization to chromatin,
516 however it did cause a hypomorphic phenotype for GC and CO frequency outcome (Figs. 2, 3).
517 This could mean that the shortened HORMA domain in Hop1-sv2 is still (partially?) functional,
518 and/or that fission yeast Hop1 can be recruited or bind to chromatin in a HORMA domain-
519 independent fashion, e.g. via its CxxC Zn-finger domain (Kironmai et al. 1998) (Fig. 1).
520 It is very interesting how genetic pathways driving meiotic chromosome organization and
521 meiotic recombination are rewired during evolution. The fission yeast, which is lacking a
522 synaptonemal complex, but retains remnants of a meiosis-specific chromosome axis, is a great
523 model for probing the roles of conserved meiotic factors such as Hop1. Clearly, Hop1 fulfills
524 an important meiotic function in promoting DSB formation and inter-homolog recombination

525 in this organism, but lacks regulatory roles in lieu of the synaptonemal complex, which appears
526 crucial in the majority of organisms performing meiosis with a synaptonemal complex.
527
528 **Acknowledgments**
529 We are grateful to Shin-ichiro Hiraga, Franz Klein, Jürg Kohli, Walter W. Steiner, Matthew C.
530 Whitby, and the National BioResource Project (NBRP) Japan for providing strains and/or
531 plasmids, and to K.C. Chan, M. Roca, and D. Whyte for technical assistance. Kevin Corbett,
532 Nancy Hollingsworth, Takashi Kubota, and Josef Loidl are thanked for critical reading of this
533 manuscript. Microscopy was performed at the University of Aberdeen Microscopy & Histology
534 facility (Kevin Mackenzie). This work was supported by the Biotechnology and Biological
535 Sciences Research Council UK (BBSRC, Doctoral Training Grant BB/F016964/1), and the
536 University of Aberdeen (College of Life Sciences and Medicine Start-up grant to AL).
537
538 **Author contributions**
539 SDB: unpublished essential reagents (yeast strains, plasmids), acquisition of data, analysis and
540 interpretation of data, revising the manuscript; ODJ: acquisition of data, revising the
541 manuscript; AL: conception and design, unpublished essential reagents (yeast strains,
542 plasmids), acquisition of data, analysis and interpretation of data, drafting and revising the
543 manuscript.

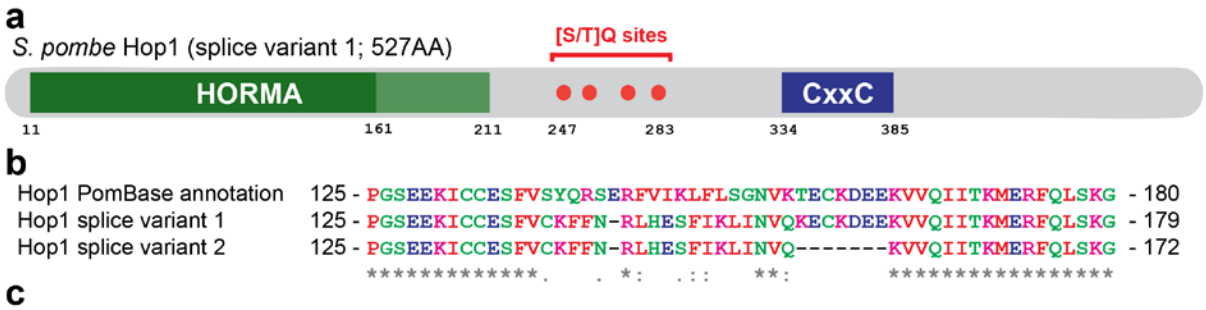

	splice variant 1 (sv1)	splice variant 2 (sv2)	aberrant	total
UoA399 (5h)	14	1	1	16
UoA722 (4h)	3	0	0	3
UoA722 (5h)	3	0	0	3
UoA722 (6h)	3	0	0	3

Figure 1. *Schizosaccharomyces pombe* Hop1 domain structure and alignment between annotated and experimentally determined versions. (**a**) Schematic of the domain structure of the experimentally derived sv1 (splice variant 1) version of Hop1 with the HORMA domain at the N terminus (AAs 11-211), four potential [S/T]Q phosphorylation sites (red dots) distributed between AAs 247 to 283, and residues 334-385 comprising the CxxC Zn-finger domain (dark blue). The HORMA domain can be subdivided into a core domain (dark green) represented by the most C-terminal ~150 AAs and a "safety-belt" region (light green; residues 161-211) (Rosenberg and Corbett 2015). Positions of key AA residues are indicated below the schematic. (**b**) ClustalΩ alignment (Sievers et al. 2014) of part of the HORMA domain (starting at residue 125) of the current PomBase-annotation of Hop1, and the two observed splice variants Hop1-sv1 and Hop1-sv2. Colouring of AAs follows the standard ClustalΩ scheme according to physicochemical properties: red for small and small & hydrophobic AAs (AVFPMILW); blue for acidic AAs (DE); magenta for basic AAs (RK); and green for AAs containing hydroxyl-, sulfhydryl-, or amine-groups. Consensus symbols below the alignment indicate full conservation (*) and conservation of groups with strongly similar (:) or weakly similar (.) properties, for details see http://www.ebi.ac.uk/Tools/msa/clustalo/help/faq.html.

561 (**c**) Relative abundance of different *hop1* splice variants found in cDNA of the indicated diploid

562 strains at given time-points of a meiotic time-course.

563

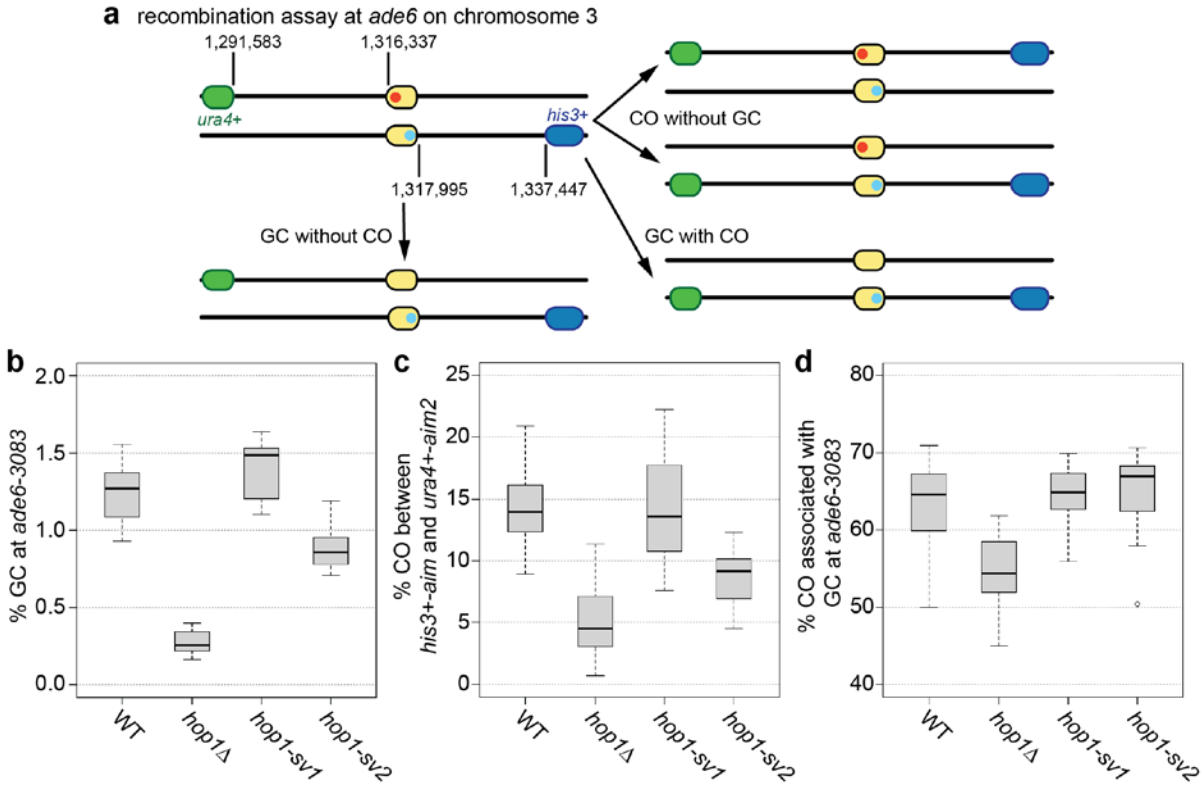

564

565 **Figure 2. Wild-type and *hop1* mutant levels of meiotic recombination at the *ade6-3083***

566 **hotspot.** (**a**) Schematic of the recombination assay at *ade6* (yellow) and its prevalent

567 outcomes: positions of *ade6* and the artificially introduced markers *ura4*$^{+}$*-aim2* (green) and

568 *his3*$^{+}$*-aim* (blue) on chromosome III are given in bp; positions of the point mutations in *ade6*

569 in the two parental strains are indicated in red (*ade6-3083*) and light blue (*ade6-469*). (**b**)

570 Frequency of gene conversion (GC) at *ade6-3083*, (**c**) frequency of crossovers (COs) between

571 *ura4*$^{+}$*-aim2* and *his3*$^{+}$*-aim*, and (**d**) percentage of COs between *ura4*$^{+}$*-aim2* and *his3*$^{+}$*-aim*

572 associated with a GC event at *ade6-3083* in crosses of wild type (WT) ALP733×ALP731 (n = 12),

573 *hop1*Δ UoA200×UoA199 (n = 16), *hop1-sv1* UoA766×UoA767 (n = 10), and *hop1-sv2*

574 UoA853×UoA854 (n = 12); n indicates the number of independent crosses (see also Table S1).

575

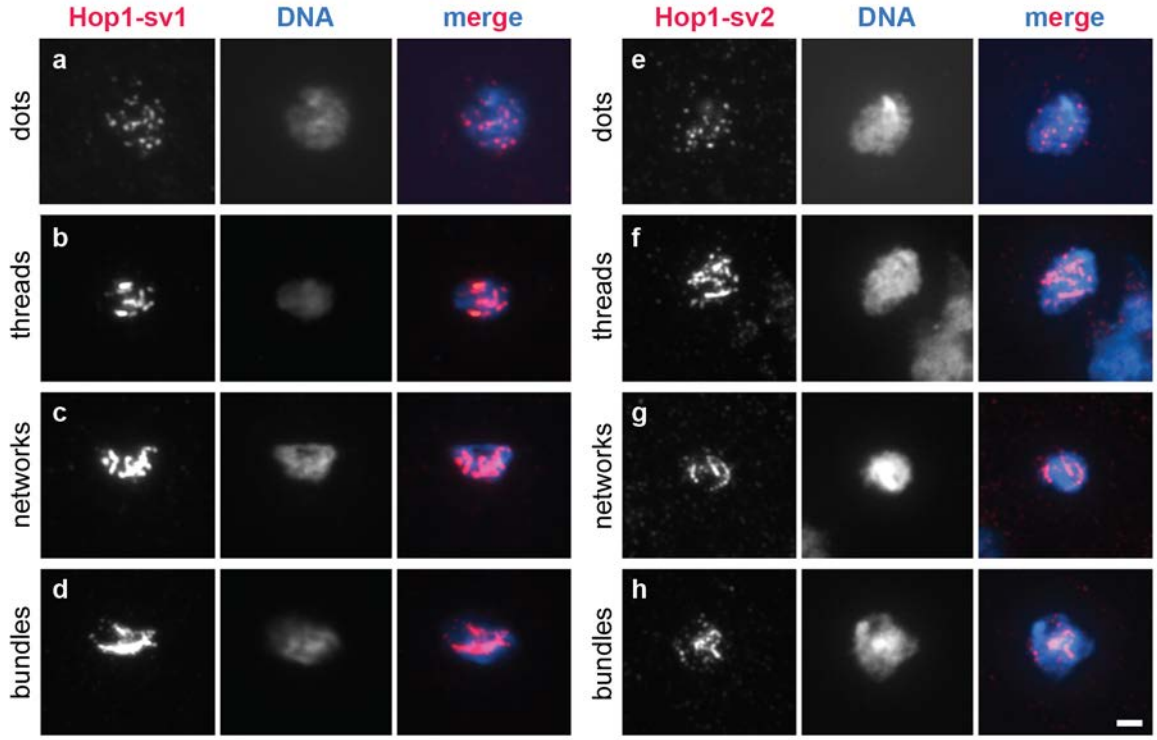

576

577 **Figure 3. Linear element morphology delineated by immunostaining of Hop1-13myc on**

578 **chromatin spreads from meiotic fission yeast cells.** Linear elements as seen by

579 immunostaining against Hop1-13myc develop from dots via threads to networks and bundles

580 in h^{+N}/h^{-smt0} *hop1-sv1/hop1-sv1::13myc-kanMX6 ade6-M210/ade6-M216* (UoA878) (**a**-**d**) or

581 h^{+N}/h^{-smt0} *hop1-sv2/hop1-sv2::13myc-kanMX6 ade6-M210/ade6-M216* (UoA930) (**e**-**h**). Hop1-

582 13myc is shown in red and Hoechst 33342-stained DNA in blue in the merge panels. Scale bar

583 represents 2 μm.

584

585

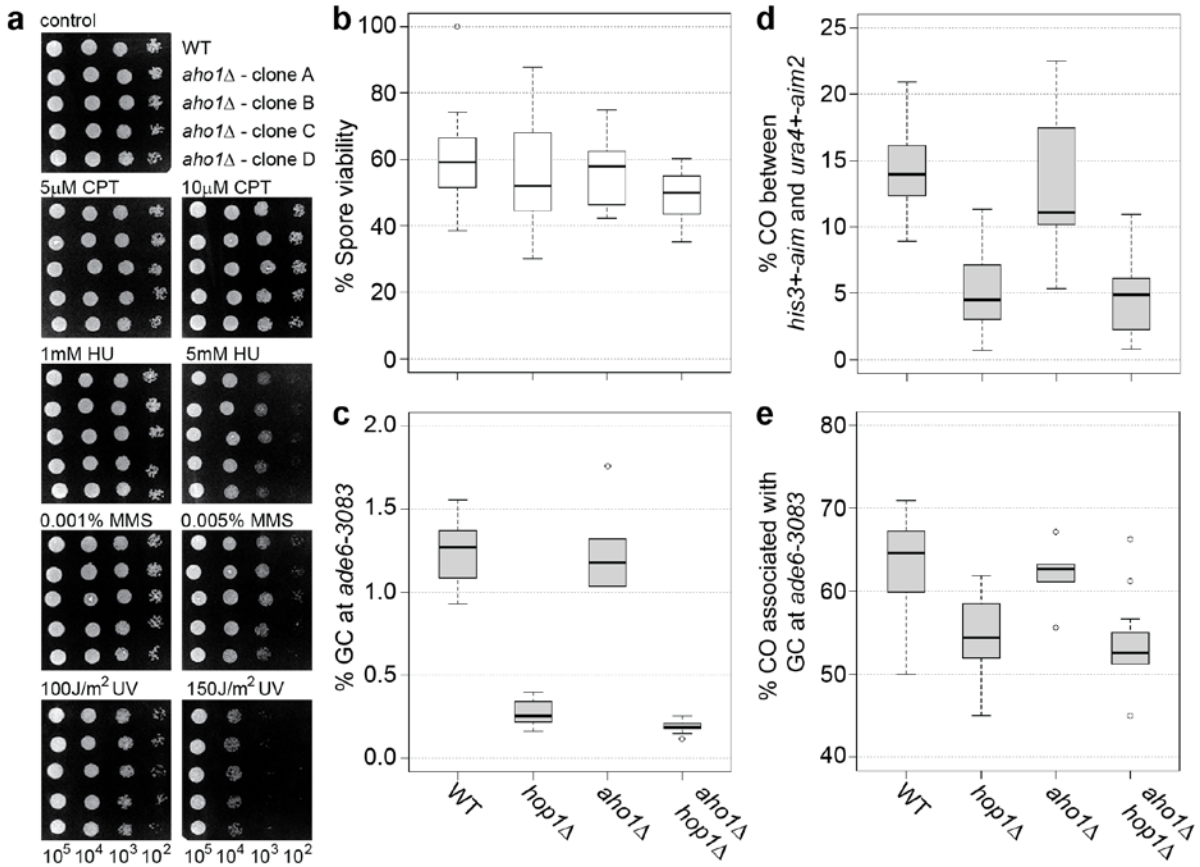

Figure 4. The role of *aho1*⁺ in genotoxic stress resistance and meiotic recombination. (**a**) Spot assays comparing wild type (WT, FO652) and *aho1*Δ (UoA423) for sensitivity to a range of genotoxins; number of cells plated in each spot is indicated at the bottom of the figure. (**b**) Percent spore viability, (**c**) frequency of gene conversion (GC) at *ade6-3083*, (**d**) frequency of crossovers (COs) between *ura4*⁺*-aim2* and *his3*⁺*-aim*, and (**e**) percentage of COs between *ura4*⁺*-aim2* and *his3*⁺*-aim* associated with a GC event at *ade6-3083* in crosses of wild type (WT) ALP733×ALP731 (n = 12), *hop1*Δ UoA200×UoA199 (n = 16), *aho1*Δ UoA424×UoA427 (n = 6), and *aho1*Δ *hop1*Δ UoA785×UoA786 (n = 13); n indicates the number of independent crosses (see also Table S1).

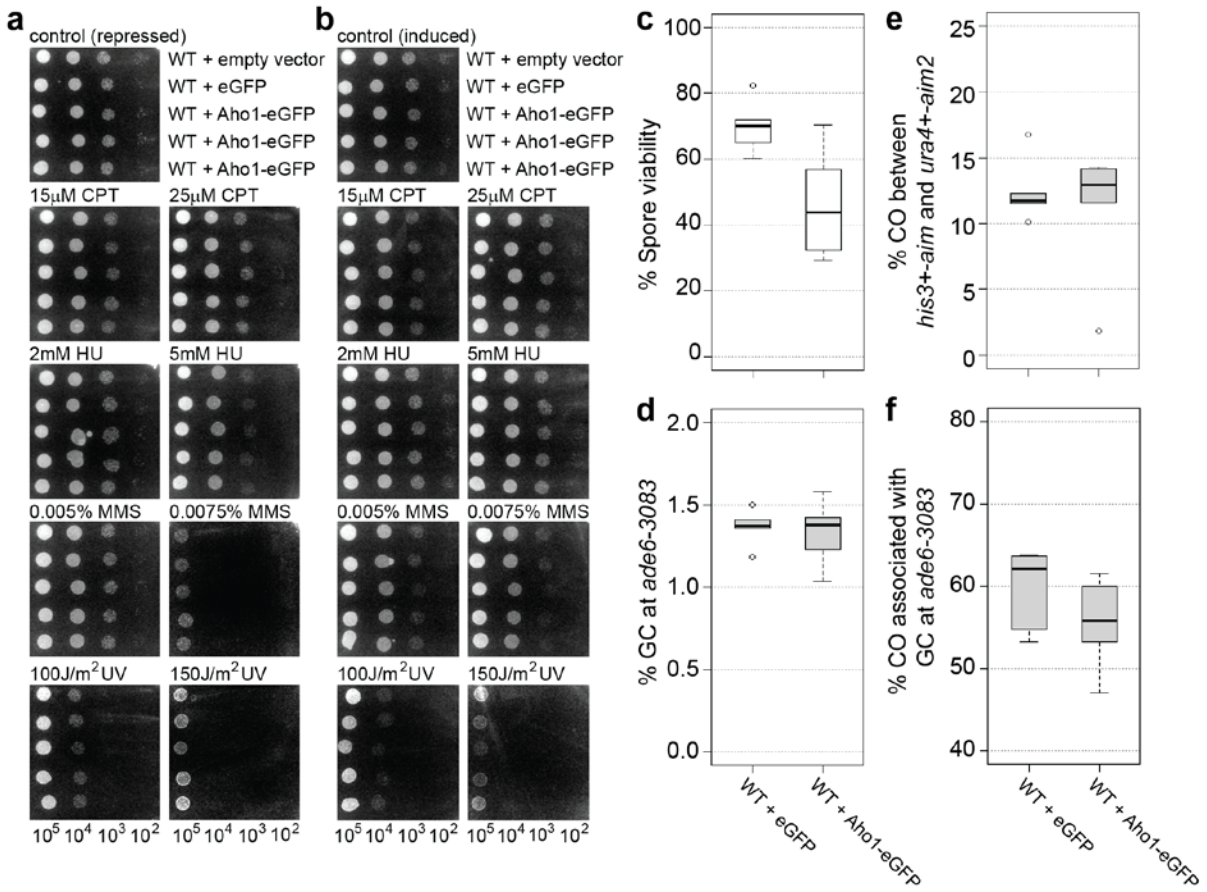

Figure 5. Over-expression of the *aho1*⁺ in wild-type fission yeast cells and its consequences for genotoxic stress resistance and meiotic recombination. (**a**, **b**) Effect of GFP and Aho1-GFP over-expression on the genotoxin sensitivity of wild type (WT, FO652); number of cells plated in each spot is indicated at the bottom of the figure. (**c**) Percent spore viability, (**d**) frequency of gene conversion (GC) at *ade6-3083*, (**e**) frequency of crossovers (COs) between *ura4*⁺-*aim2* and *his3*⁺-*aim*, and (**f**) percentage of COs between *ura4*⁺-*aim2* and *his3*⁺-*aim* associated with a GC event at *ade6-3083* in crosses of wild type (WT) ALP733×UoA841 over-expressing GFP (n = 6), or Aho1-GFP (n = 6); n indicates the number of independent crosses (see also Table S2).

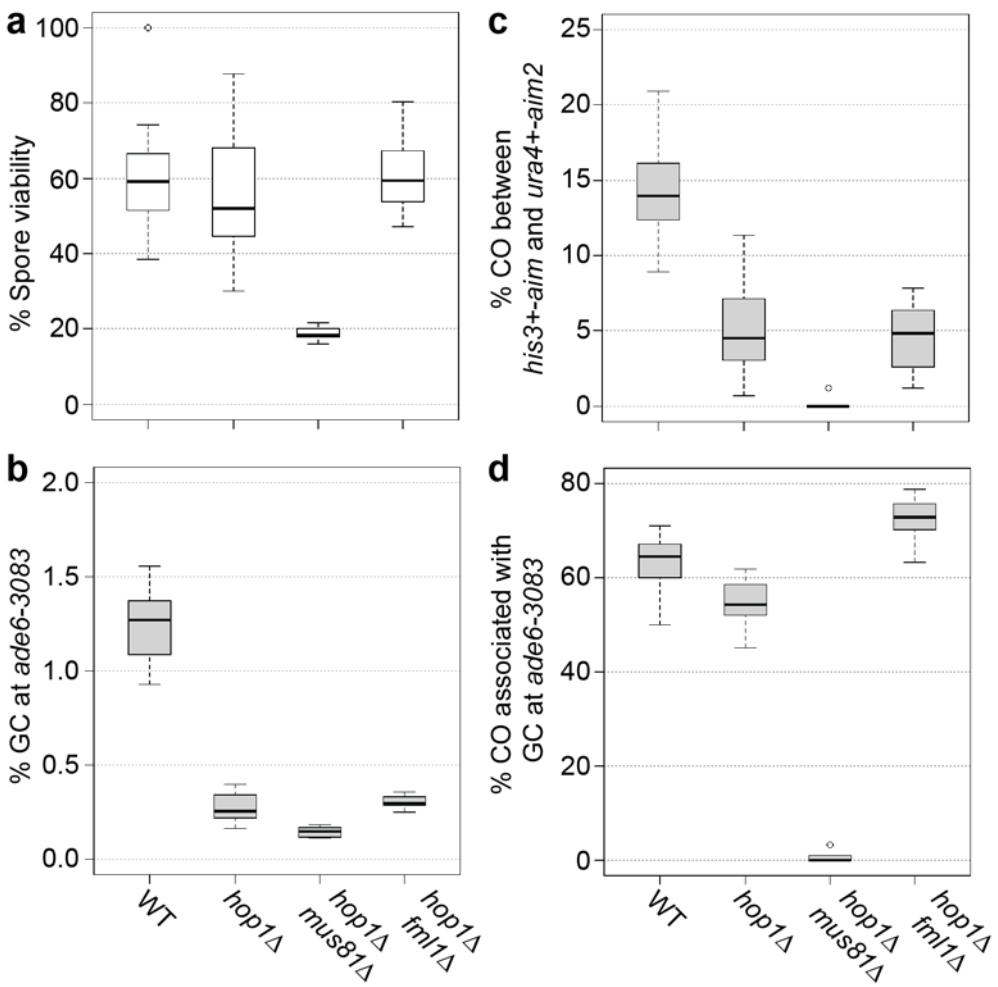

607

608 **Figure 6. Genetic interaction of *hop1*Δ with deletions of factors required for meiotic**
609 **recombination intermediate processing.** (**a**) Percent spore viability, (**b**) frequency of gene
610 conversion (GC) at *ade6-3083*, (**c**) frequency of crossovers (COs) between *ura4*$^{+}$*-aim2* and
611 *his3*$^{+}$*-aim*, and (**d**) percentage of COs between *ura4*$^{+}$*-aim2* and *his3*$^{+}$*-aim* associated with a GC
612 event at *ade6-3083* in crosses of wild type (WT) ALP733×ALP731 (n = 12), *hop1*Δ
613 UoA200×UoA199 (n = 16), *hop1*Δ *mus81*Δ UoA204×UoA203 (n = 6), and *fml1*Δ *hop1*Δ
614 UoA182×UoA181 (n = 14); n indicates the number of independent crosses (see also Table S1).
615

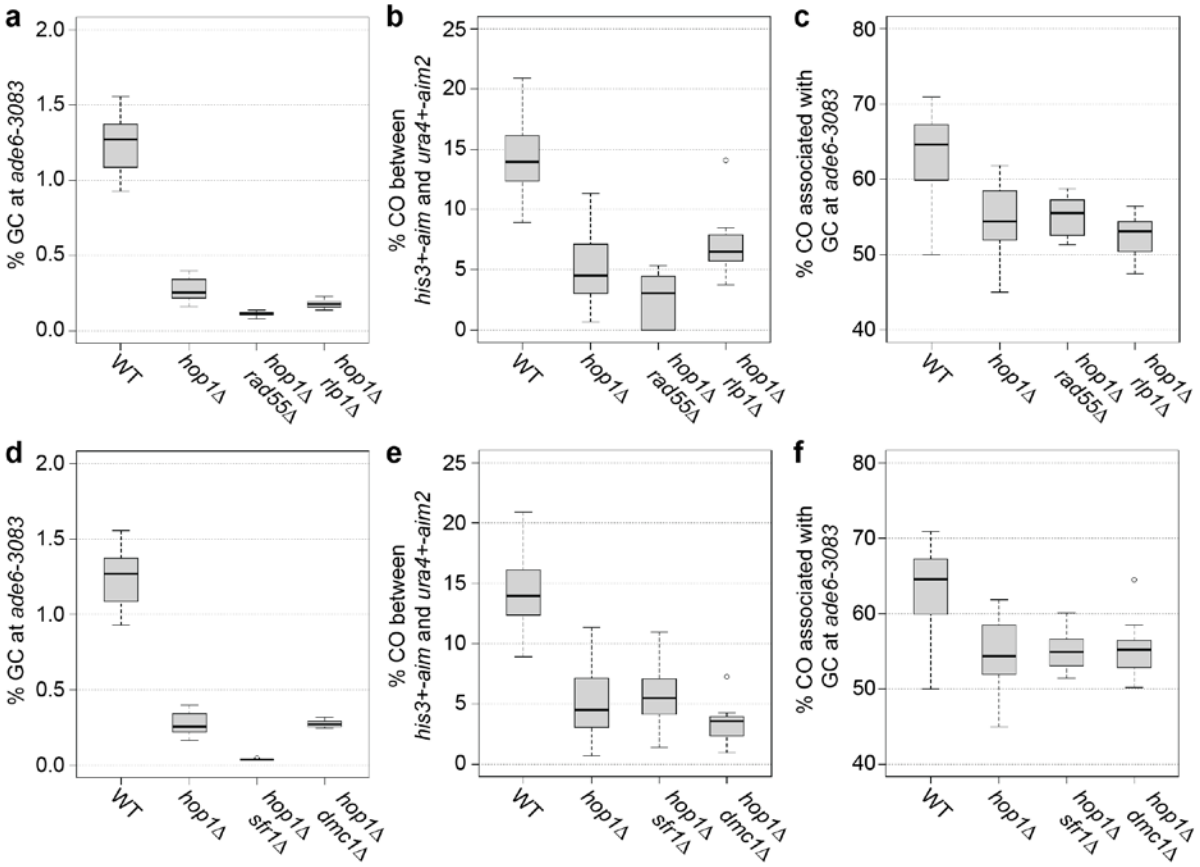

616

617 **Figure 7. Genetic interaction of *hop1*Δ with deletions of Rad51/Dmc1-mediator genes.** (**a**, **d**)
618 frequency of gene conversion (GC) at *ade6-3083*, (**b**, **e**) frequency of crossovers (COs) between
619 *ura4*$^{+}$*-aim2* and *his3*$^{+}$*-aim*, and (**c**,**f**) percentage of COs between *ura4*$^{+}$*-aim2* and *his3*$^{+}$*-aim*
620 associated with a GC event at *ade6-3083* in crosses of wild type (WT) ALP733×ALP731 (n = 12),
621 *hop1*Δ UoA200×UoA199 (n = 16), *hop1*Δ *rad55*Δ UoA846×UoA847 (n = 10), *hop1*Δ *rlp1*Δ
622 UoA848×UoA849 (n = 10), *hop1*Δ *sfr1*Δ UoA844×UoA845 (n = 12), and
623 *dmc1*Δ *hop1*Δ UoA851×UoA852 (n = 10); n indicates the number of independent crosses (see
624 also Table S1).

625

626

627 **Table 1.** Yeast strain list (in order of appearance)

Strain	Relevant genotype	Origin
UoA399	*h^{+S}/h^{-smt0} atb2^{+}/GFP-atb2^{+}::natMX4 mug20^{+}/mug20^{+}::GFP-kanMX6 uch2^{+}/uch2^{+}::mCHERRY-ura4+ ade6-M210/ade6-M216 ura4-D18/ura4-D18*	lab strain
UoA722	*h^{+N}/h^{-} rad11^{+}::GFP-kanMX6/rad11^{+} ade6-M210/ade6-M216*	lab strain
ALP733	*h^{+S} ade6-3083 ura4^{+}-aim2 his3-D1 leu1-32 ura4-D18*	(Lorenz et al. 2010)
ALP731	*h^{-smt0} ade6-469 his3^{+}-aim arg3-D4 his3-D1 ura4-D18*	(Lorenz et al. 2010)
UoA200	*h^{+S} hop1Δ-25::natMX6 ade6-3083 ura4^{+}-aim2 his3-D1 leu1-32 ura4-D18*	this study
UoA199	*h^{-smt0} hop1Δ-25::natMX6 ade6-469 his3^{+}-aim arg3-D4 his3-D1 ura4-D18*	this study
UoA766	*h^{+S} hop1-sv1 ade6-3083 ura4^{+}-aim2 his3-D1 leu1-32 ura4-D18*	this study
UoA767	*h^{-smt0} hop1-sv1 ade6-469 his3^{+}-aim arg3-D4 his3-D1 ura4-D18*	this study
UoA853	*h^{+S} hop1-sv2 ade6-3083 ura4^{+}-aim2 his3-D1 leu1-32 ura4-D18*	this study
UoA854	*h^{-smt0} hop1-sv2 ade6-469 his3^{+}-aim arg3-D4 his3-D1 ura4-D18*	this study
UoA863	*h^{+N} hop1-sv1 ade6-M210*	this study
UoA866	*h^{-smt0} hop1-sv1::13myc-kanMX6 ade6-M216*	this study
UoA868	*h^{+N} hop1-sv2 ade6-M210*	this study
UoA929	*h^{-smt0} hop1-sv2::13myc-kanMX6 ade6-M216*	this study
UoA878	*h^{+N}/h^{-smt0} hop1-sv1/hop1-sv1::13myc-kanMX6 ade6-M210/ade6-M216*	this study; (UoA863xUoA866)
UoA930	*h^{+N}/h^{-smt0} hop1-sv2/hop1-sv2::13myc-kanMX6 ade6-M210/ade6-M216*	this study; (UoA868xUoA929)
FO652	*h^{-smt0} arg3-D4 his3-D1 leu1-32 ura4-D18*	lab strain; (Lorenz et al. 2014)
UoA423	*h^{-smt0} aho1Δ-84::natMX4 arg3-D4 his3-D1 leu1-32 ura4-D18*	this study
UoA424	*h^{+S} aho1Δ-84::natMX4 ade6-3083 ura4^{+}-aim2 his3-D1 leu1-32 ura4-D18*	this study
UoA427	*h^{-smt0} aho1Δ-84::natMX4 ade6-469 his3^{+}-aim arg3-D4 his3-D1 ura4-D18*	this study
UoA786	*h^{+S} aho1Δ-84::natMX4 hop1Δ-1::kanMX6 ade6-3083 ura4^{+}-aim2 his3-D1 leu1-32 ura4-D18*	this study
UoA785	*h^{-smt0} aho1Δ-84::natMX4 hop1Δ-1::kanMX6 ade6-469 his3^{+}-aim arg3-D4 his3-D1 ura4-D18*	this study
UoA841	*h^{-smt0} ade6-469 his3^{+}-aim his3-D1 leu1-32 ura4-D18*	this study
UoA204	*h^{+S} hop1Δ-25::natMX6 mus81Δ::kanMX6 ade6-3083 ura4^{+}-aim2 his3-D1 leu1-32 ura4-D18*	this study
UoA203	*h^{-smt0} hop1Δ-25::natMX6 mus81Δ::kanMX6 ade6-469 his3^{+}-aim arg3-D4 his3-D1 ura4-D18*	this study
UoA182	*h^{+S} fml1Δ::hphMX4 hop1Δ-25::natMX6 ade6-3083 ura4^{+}-aim2 his3-D1 leu1-32 ura4-D18*	this study
UoA181	*h^{-smt0} fml1Δ::hphMX4 hop1Δ-25::natMX6 ade6-469 his3^{+}-aim arg3-D4 his3-D1 ura4-D18*	this study
UoA847[a]	*h^{+S} hop1Δ-25::natMX6 rad55Δ::hphMX4 ade6-469 his3^{+}-aim arg3-D4 his3-D1 ura4-D18*	this study
UoA846[a]	*h^{-smt0} hop1Δ-25::natMX6 rad55Δ::hphMX4 ade6-3083 ura4^{+}-aim2 his3-D1 leu1-32 ura4-D18*	this study
UoA849	*h^{+N} hop1Δ-25::natMX6 rlp1Δ::kanMX6 ade6-469 his3^{+}-aim arg3-D4 his3-D1 ura4-D18*	this study
UoA848	*h^{-smt0} hop1Δ-25::natMX6 rlp1Δ::kanMX6 ade6-3083 ura4^{+}-aim2 his3-D1 leu1-32 ura4-D18*	this study
UoA845	*h^{+S} hop1Δ-25::natMX6 sfr1Δ-11::hphMX4 ade6-469 his3^{+}-aim arg3-D4 his3-D1 ura4-D18*	this study
UoA844	*h^{-smt0} hop1Δ-25::natMX6 sfr1Δ-11::hphMX4 ade6-3083 ura4^{+}-aim2 his3-D1 leu1-32 ura4-D18*	this study
UoA852	*h^{+S} dmc1Δ-25::kanMX6 hop1Δ-25::natMX6 ade6-3083 ura4^{+}-aim2 his3-D1 leu1-32 ura4-D18*	this study
UoA851	*h^{-smt0} dmc1Δ-25::kanMX6 hop1Δ-25::natMX6 ade6-469 his3^{+}-aim arg3-D4 his3-D1 ura4-D18*	this study
UoA473	*h^{-} ade6-149*	lab strain
ALP1594	*h^{-smt0} ade7-50 arg3-D4 his3-D1 ura4-D18*	lab strain
ALP1596	*h^{-smt0} ade7-152 his3-D1 leu1-32 ura4-D18*	lab strain; (Lorenz et al. 2014)
UoA725	*h^{-smt0} hop1-3::ura4^{+} arg3-D4 his3-D1 leu1-32 ura4-D18*	this study
UoA746	*h^{-smt0} hop1-sv1 arg3-D4 his3-D1 leu1-32 ura4-D18*	this study
UoA747	*h^{-smt0} hop1-sv2 arg3-D4 his3-D1 leu1-32 ura4-D18*	this study
UoA782	*h^{-smt0} hop1-sv1::13myc-kanMX6 arg3-D4 his3-D1 leu1-32 ura4-D18*	this study
UoA927	*h^{+N} hop1-sv2::13myc-kanMX6 ade6-M210*	this study

628 [a]strains are derivatives of FY18530 provided by the National BioResource Project (NBRP) of the MEXT, Japan.

629 **References**

630 Akamatsu Y, Dziadkowiec D, Ikeguchi M, et al (2003) Two different Swi5-containing protein
631 complexes are involved in mating-type switching and recombination repair in fission
632 yeast. Proc Natl Acad Sci U S A 100:15770–5. doi: 10.1073/pnas.2632890100

633 Andreoletti G, Seaby EG, Dewing JM, et al (2017) *AMMECR1*: a single point mutation causes
634 developmental delay, midface hypoplasia and elliptocytosis. J Med Genet 54:269–277.
635 doi: 10.1136/jmedgenet-2016-104100

636 Aravind L, Koonin E V (1998) The HORMA domain: a common structural denominator in
637 mitotic checkpoints, chromosome synapsis and DNA repair. Trends Biochem Sci 23:284–
638 6. doi: 10.1016/S0968-0004(98)01257-2

639 Armstrong SJ, Caryl AP, Jones GH, Franklin FCH (2002) Asy1, a protein required for meiotic
640 chromosome synapsis, localizes to axis-associated chromatin in *Arabidopsis* and
641 *Brassica*. J Cell Sci 115:3645–55. doi: 10.1242/jcs.00048

642 Bähler J, Wu JQ, Longtine MS, et al (1998) Heterologous modules for efficient and versatile
643 PCR-based gene targeting in *Schizosaccharomyces pombe*. Yeast 14:943–51. doi:
644 10.1002/(SICI)1097-0061(199807)14:10<943::AID-YEA292>3.0.CO;2-Y

645 Bähler J, Wyler T, Loidl J, Kohli J (1993) Unusual nuclear structures in meiotic prophase of
646 fission yeast: a cytological analysis. J Cell Biol 121:241–56.

647 Bishop DK, Park D, Xu L, Kleckner N (1992) *DMC1*: a meiosis-specific yeast homolog of E. coli
648 *recA* required for recombination, synaptonemal complex formation, and cell cycle
649 progression. Cell 69:439–56.

650 Bleuyard J-Y, Gallego ME, Savigny F, White CI (2005) Differing requirements for the
651 Arabidopsis Rad51 paralogs in meiosis and DNA repair. Plant J 41:533–45. doi:
652 10.1111/j.1365-313X.2004.02318.x

653 Brown MS, Bishop DK (2014) DNA strand exchange and RecA homologs. Cold Spring Harb
654 Perspect Biol 7:1–30. doi: 10.1101/cshperspect.a016659

655 Brown SD, Lorenz A (2016) Single-step marker switching in *Schizosaccharomyces pombe*
656 using a lithium acetate transformation protocol. Bio-protocol 6:e2075. doi:
657 10.21769/BioProtoc.2075

658 Cahoon CK, Hawley RS (2016) Regulating the construction and demolition of the
659 synaptonemal complex. Nat Struct Mol Biol 23:369–377. doi: 10.1038/nsmb.3208

660 Callender TL, Laureau R, Wan L, et al (2016) Mek1 down regulates Rad51 activity during
661 yeast meiosis by phosphorylation of Hed1. PLoS Genet 12:e1006226. doi:
662 10.1371/journal.pgen.1006226

663 Carballo JA, Johnson AL, Sedgwick SG, Cha RS (2008) Phosphorylation of the axial element
664 protein Hop1 by Mec1/Tel1 ensures meiotic interhomolog recombination. Cell
665 132:758–70. doi: 10.1016/j.cell.2008.01.035

666 Caryl AP, Armstrong SJ, Jones GH, Franklin FC (2000) A homologue of the yeast *HOP1* gene is
667 inactivated in the Arabidopsis meiotic mutant *asy1*. Chromosoma 109:62–71.

668 Couteau F, Zetka M (2005) HTP-1 coordinates synaptonemal complex assembly with
669 homolog alignment during meiosis in *C. elegans*. Genes Dev 19:2744–56. doi:
670 10.1101/gad.1348205

671 Craven RA, Griffiths DJ, Sheldrick KS, et al (1998) Vectors for the expression of tagged
672 proteins in *Schizosaccharomyces pombe*. Gene 221:59–68. doi: 10.1016/S0378-
673 1119(98)00434-X

674 Daniel K, Lange J, Hached K, et al (2011) Meiotic homologue alignment and its quality
675 surveillance are controlled by mouse HORMAD1. Nat Cell Biol 13:599–610. doi:
676 10.1038/ncb2213

677 de los Santos T, Hollingsworth NM (1999) Red1p, a *MEK1*-dependent phosphoprotein that
678 physically interacts with Hop1p during meiosis in yeast. J Biol Chem 274:1783–90.

679 Doe CL, Dixon J, Osman F, Whitby MC (2000) Partial suppression of the fission yeast *rqh1*$^{-}$
680 phenotype by expression of a bacterial Holliday junction resolvase. EMBO J 19:2751–62.
681 doi: 10.1093/emboj/19.11.2751

682 Ellermeier C, Schmidt H, Smith GR (2004) Swi5 acts in meiotic DNA joint molecule formation
683 in *Schizosaccharomyces pombe*. Genetics 168:1891–8. doi:
684 10.1534/genetics.104.034280

685 Faul F, Erdfelder E, Buchner A, Lang A-G (2009) Statistical power analyses using G*Power 3.1:
686 tests for correlation and regression analyses. Behav Res Methods 41:1149–60. doi:
687 10.3758/BRM.41.4.1149

688 Faul F, Erdfelder E, Lang A-G, Buchner A (2007) G*Power: A flexible statistical power analysis
689 program for the social, behavioral, and biomedical sciences. Behav Res Methods
690 39:175–191. doi: 10.3758/BF03193146

691 Flor-Parra I, Zhurinsky J, Bernal M, et al (2014) A Lallzyme MMX-based rapid method for
692 fission yeast protoplast preparation. Yeast 31:61–6. doi: 10.1002/yea.2994

693 Fukuda T, Daniel K, Wojtasz L, et al (2010) A novel mammalian HORMA domain-containing
694 protein, HORMAD1, preferentially associates with unsynapsed meiotic chromosomes.
695 Exp Cell Res 316:158–71. doi: 10.1016/j.yexcr.2009.08.007

696 Goldstein AL, McCusker JH (1999) Three new dominant drug resistance cassettes for gene
697 disruption in *Saccharomyces cerevisiae*. Yeast 15:1541–53. doi: 10.1002/(SICI)1097-
698 0061(199910)15:14<1541::AID-YEA476>3.0.CO;2-K

699 Goodyer W, Kaitna S, Couteau F, et al (2008) HTP-3 links DSB formation with homolog
700 pairing and crossing over during *C. elegans* meiosis. Dev Cell 14:263–74. doi:
701 10.1016/j.devcel.2007.11.016

702 Gray S, Cohen PE (2016) Control of meiotic crossovers: From double-strand break formation
703 to designation. Annu Rev Genet 50:175–210. doi: 10.1146/annurev-genet-120215-
704 035111

705 Grimm C, Kohli J, Murray J, Maundrell K (1988) Genetic engineering of *Schizosaccharomyces*
706 *pombe*: a system for gene disruption and replacement using the *ura4* gene as a
707 selectable marker. Mol Gen Genet 215:81–6.

708 Grishchuk AL, Kohli J (2003) Five RecA-like proteins of *Schizosaccharomyces pombe* are
709 involved in meiotic recombination. Genetics 165:1031–43.

710 Hartsuiker E, Mizuno K, Molnar M, et al (2009) Ctp1^{CtIP} and Rad32^{Mre11} nuclease activity are
711 required for Rec12^{Spo11} removal, but Rec12^{Spo11} removal is dispensable for other MRN-
712 dependent meiotic functions. Mol Cell Biol 29:1671–81. doi: 10.1128/MCB.01182-08

713 Haruta N, Kurokawa Y, Murayama Y, et al (2006) The Swi5-Sfr1 complex stimulates
714 Rhp51/Rad51- and Dmc1-mediated DNA strand exchange in vitro. Nat Struct Mol Biol
715 13:823–30. doi: 10.1038/nsmb1136

716 Hayase A, Takagi M, Miyazaki T, et al (2004) A protein complex containing Mei5 and Sae3
717 promotes the assembly of the meiosis-specific RecA homolog Dmc1. Cell 119:927–40.
718 doi: 10.1016/j.cell.2004.10.031

719 Hollingsworth NM, Byers B (1989) *HOP1*: a yeast meiotic pairing gene. Genetics 121:445–62.

720 Hollingsworth NM, Goetsch L, Byers B (1990) The *HOP1* gene encodes a meiosis-specific
721 component of yeast chromosomes. Cell 61:73–84. doi: 10.1016/0092-8674(90)90216-2

722 Hong S, Sung Y, Yu M, et al (2013) The logic and mechanism of homologous recombination
723 partner choice. Mol Cell 51:440–453. doi: 10.1016/j.molcel.2013.08.008

724 Hunter N (2015) Meiotic recombination: the essence of heredity. Cold Spring Harb Perspect
725 Biol 7:a016618. doi: 10.1101/cshperspect.a016618

726 Hyppa RW, Smith GR (2010) Crossover invariance determined by partner choice for meiotic
727 DNA break repair. Cell 142:243–55. doi: 10.1016/j.cell.2010.05.041

728 Keeney JB, Boeke JD (1994) Efficient targeted integration at *leu1-32* and *ura4-294* in
729 *Schizosaccharomyces pombe*. Genetics 136:849–56.

730 Khan K, Madhavan TPV, Kshirsagar R, et al (2013) N-terminal disordered domain of
731 *Saccharomyces cerevisiae* Hop1 protein is dispensable for DNA binding, bridging, and
732 synapsis of double-stranded DNA molecules but is necessary for spore formation.
733 Biochemistry 52:5265–79. doi: 10.1021/bi4005528

734 Kim Y, Rosenberg SC, Kugel CL, et al (2014) The chromosome axis controls meiotic events
735 through a hierarchical assembly of HORMA domain proteins. Dev Cell 31:487–502. doi:
736 10.1016/j.devcel.2014.09.013

737 Kironmai KM, Muniyappa K, Friedman DB, et al (1998) DNA-binding activities of Hop1
738 protein, a synaptonemal complex component from *Saccharomyces cerevisiae*. Mol Cell
739 Biol 18:1424–35.

740 Kogo H, Tsutsumi M, Ohye T, et al (2012) HORMAD1-dependent checkpoint/surveillance
741 mechanism eliminates asynaptic oocytes. Genes to Cells 17:439–54. doi:
742 10.1111/j.1365-2443.2012.01600.x

743 Lam I, Keeney S (2015) Mechanism and regulation of meiotic recombination initiation. Cold
744 Spring Harb Perspect Biol 7:a016634. doi: 10.1101/cshperspect.a016634

745 Latypov V, Rothenberg M, Lorenz A, et al (2010) Roles of Hop1 and Mek1 in meiotic
746 chromosome pairing and recombination partner choice in *Schizosaccharomyces pombe*.
747 Mol Cell Biol 30:1570–81. doi: 10.1128/MCB.00919-09

748 Loidl J (2016) Conservation and variability of meiosis across the eukaryotes. Annu Rev Genet
749 50:293–316. doi: 10.1146/annurev-genet-120215-035100

750 Loidl J (2006) *S. pombe* linear elements: the modest cousins of synaptonemal complexes.
751 Chromosoma 115:260–71. doi: 10.1007/s00412-006-0047-7

752 Loidl J, Klein F, Scherthan H (1994) Homologous pairing is reduced but not abolished in
753 asynaptic mutants of yeast. J Cell Biol 125:1191–200.

754 Loidl J, Lorenz A (2009) Analysis of *Schizosaccharomyces pombe* meiosis by nuclear
755 spreading. Methods Mol Biol 558:15–36. doi: 10.1007/978-1-60761-103-5_2

756 Lorenz A (2017a) Modulation of meiotic homologous recombination by DNA helicases. Yeast
757 34:195–203. doi: 10.1002/yea.3227

758 Lorenz A (2015) New cassettes for single-step drug resistance and prototrophic marker
759 switching in fission yeast. Yeast 32:703–710. doi: 10.1002/yea.3097

760 Lorenz A (2017b) Supporting Online Material - Genetic interactions between the
761 chromosome axis-associated protein Hop1 and homologous recombination
762 determinants in *Schizosaccharomyces pombe*. doi: 10.6084/m9.figshare.5373163

763 Lorenz A, Estreicher A, Kohli J, Loidl J (2006) Meiotic recombination proteins localize to linear
764 elements in *Schizosaccharomyces pombe*. Chromosoma 115:330–40. doi:
765 10.1007/s00412-006-0053-9

766 Lorenz A, Mehats A, Osman F, Whitby MC (2014) Rad51/Dmc1 paralogs and mediators
767 oppose DNA helicases to limit hybrid DNA formation and promote crossovers during
768 meiotic recombination. Nucleic Acids Res 42:13723–13735. doi: 10.1093/nar/gku1219

769 Lorenz A, Osman F, Folkyte V, et al (2009) Fbh1 limits Rad51-dependent recombination at
770 blocked replication forks. Mol Cell Biol 29:4742–56. doi: 10.1128/MCB.00471-09

771 Lorenz A, Osman F, Sun W, et al (2012) The fission yeast FANCM ortholog directs non-
772 crossover recombination during meiosis. Science 336:1585–8. doi:
773 10.1126/science.1220111

774 Lorenz A, Wells JL, Pryce DW, et al (2004) *S. pombe* meiotic linear elements contain proteins
775 related to synaptonemal complex components. J Cell Sci 117:3343–51. doi:
776 10.1242/jcs.01203

777 Lorenz A, West SC, Whitby MC (2010) The human Holliday junction resolvase GEN1 rescues
778 the meiotic phenotype of a *Schizosaccharomyces pombe mus81* mutant. Nucleic Acids
779 Res 38:1866–73. doi: 10.1093/nar/gkp1179

780 Martín V, Chahwan C, Gao H, et al (2006) Sws1 is a conserved regulator of homologous
781 recombination in eukaryotic cells. EMBO J 25:2564–74. doi: 10.1038/sj.emboj.7601141

782 Martinez-Perez E, Villeneuve AM (2005) HTP-1-dependent constraints coordinate homolog
783 pairing and synapsis and promote chiasma formation during *C. elegans* meiosis. Genes
784 Dev 19:2727–43. doi: 10.1101/gad.1338505

785 Mata J, Lyne R, Burns G, Bähler J (2002) The transcriptional program of meiosis and
786 sporulation in fission yeast. Nat Genet 32:143–7. doi: 10.1038/ng951

787 Matsuyama A, Arai R, Yashiroda Y, et al (2006) ORFeome cloning and global analysis of
788 protein localization in the fission yeast *Schizosaccharomyces pombe*. Nat Biotechnol
789 24:841–7. doi: 10.1038/nbt1222

790 Mimitou EP, Symington LS (2011) DNA end resection-Unraveling the tail. DNA Repair (Amst)
791 10:344–348. doi: 10.1016/j.dnarep.2010.12.004

792 Molnar M (2003) Linear element formation and their role in meiotic sister chromatid
793 cohesion and chromosome pairing. J Cell Sci 116:1719–1731. doi: 10.1242/jcs.00387

794 Moreno MB, Durán A, Ribas JC (2000) A family of multifunctional thiamine-repressible
795 expression vectors for fission yeast. Yeast 16:861–72. doi: 10.1002/1097-

796 0061(20000630)16:9<861::AID-YEA577>3.0.CO;2-9

797 Neale MJ, Pan J, Keeney S (2005) Endonucleolytic processing of covalent protein-linked DNA
798 double-strand breaks. Nature 436:1053–7. doi: 10.1038/nature03872

799 Niu H, Wan L, Baumgartner B, et al (2005) Partner choice during meiosis is regulated by
800 Hop1-promoted dimerization of Mek1. Mol Biol Cell 16:5804–18. doi:
801 10.1091/mbc.E05-05-0465

802 Niu H, Wan L, Busygina V, et al (2009) Regulation of meiotic recombination via Mek1-
803 mediated Rad54 phosphorylation. Mol Cell 36:393–404. doi:
804 10.1016/j.molcel.2009.09.029

805 Olson LW, Eden U, Egel-Mitani M, Egel R (1978) Asynaptic meiosis in fission yeast? Hereditas
806 89:189–199. doi: 10.1111/j.1601-5223.1978.tb01275.x

807 Osman F, Dixon J, Doe CL, Whitby MC (2003) Generating crossovers by resolution of nicked
808 Holliday junctions: a role for Mus81-Eme1 in meiosis. Mol Cell 12:761–74. doi:
809 10.1016/S1097-2765(03)00343-5

810 Pancaldi V, Saraç OS, Rallis C, et al (2012) Predicting the fission yeast protein interaction
811 network. G3 (Bethesda) 2:453–67. doi: 10.1534/g3.111.001560

812 Phadnis N, Cipak L, Polakova S, et al (2015) Casein kinase 1 and phosphorylation of cohesin
813 subunit Rec11 (SA3) promote meiotic recombination through linear element formation.
814 PLoS Genet 11:e1005225. doi: 10.1371/journal.pgen.1005225

815 Rinaldi VD, Bolcun-Filas E, Kogo H, et al (2017) The DNA damage checkpoint eliminates
816 mouse oocytes with chromosome synapsis failure. Mol Cell
817 10.1016/j.molcel.2017.07.027. doi: 10.1016/j.molcel.2017.07.027

818 Rosenberg SC, Corbett KD (2015) The multifaceted roles of the HORMA domain in cellular
819 signaling. J Cell Biol 211:745–55. doi: 10.1083/jcb.201509076

820 Rothenberg M, Kohli J, Ludin K (2009) Ctp1 and the MRN-complex are required for
821 endonucleolytic Rec12 removal with release of a single class of oligonucleotides in
822 fission yeast. PLoS Genet 5:e1000722. doi: 10.1371/journal.pgen.1000722

823 Sabatinos SA, Forsburg SL (2010) Molecular genetics of *Schizosaccharomyces pombe*.
824 Methods Enzymol 470:759–95. doi: 10.1016/S0076-6879(10)70032-X

825 Sakuno T, Watanabe Y (2015) Phosphorylation of cohesin Rec11/SA3 by Casein Kinase 1
826 promotes homologous recombination by assembling the meiotic chromosome axis. Dev
827 Cell 32:220–230. doi: 10.1016/j.devcel.2014.11.033

828 Sambrook JF, Russell DW (2000) Molecular Cloning: A Laboratory Manual, 3rd edn. Cold
829 Spring Harbor Laboratory Press, Cold Spring Harbor

830 Sanchez-Moran E, Santos J-L, Jones GH, Franklin FCH (2007) ASY1 mediates AtDMC1-
831 dependent interhomolog recombination during meiosis in *Arabidopsis*. Genes Dev
832 21:2220–33. doi: 10.1101/gad.439007

833 Sasanuma H, Tawaramoto MS, Lao JP, et al (2013) A new protein complex promoting the
834 assembly of Rad51 filaments. Nat Commun 4:1676. doi: 10.1038/ncomms2678

835 Sato M, Dhut S, Toda T (2005) New drug-resistant cassettes for gene disruption and epitope
836 tagging in *Schizosaccharomyces pombe*. Yeast 22:583–91. doi: 10.1002/yea.1233

837 Schwacha A, Kleckner N (1997) Interhomolog bias during meiotic recombination: meiotic
838 functions promote a highly differentiated interhomolog-only pathway. Cell 90:1123–35.

839 Shinohara A, Gasior S, Ogawa T, et al (1997) *Saccharomyces cerevisiae recA* homologues
840 *RAD51* and *DMC1* have both distinct and overlapping roles in meiotic recombination.
841 Genes to Cells 2:615–29. doi: 10.1046/j.1365-2443.1997.1480347.x

842 Sievers F, Wilm A, Dineen D, et al (2014) Fast, scalable generation of high-quality protein
843 multiple sequence alignments using Clustal Omega. Mol Syst Biol 7:539–539. doi:
844 10.1038/msb.2011.75

845 Silva N, Ferrandiz N, Barroso C, et al (2014) The fidelity of synaptonemal complex assembly is
846 regulated by a signaling mechanism that controls early meiotic progression. Dev Cell
847 31:503–511. doi: 10.1016/j.devcel.2014.10.001

848 Smith GR (2009) Genetic analysis of meiotic recombination in *Schizosaccharomyces pombe*.
849 Methods Mol Biol 557:65–76. doi: 10.1007/978-1-59745-527-5_6

850 Smith GR, Boddy MN, Shanahan P, Russell P (2003) Fission yeast Mus81.Eme1 Holliday
851 junction resolvase is required for meiotic crossing over but not for gene conversion.
852 Genetics 165:2289–93.

853 Smith A V, Roeder GS (1997) The yeast Red1 protein localizes to the cores of meiotic
854 chromosomes. J Cell Biol 136:957–67.

855 Spirek M, Estreicher A, Csaszar E, et al (2010) SUMOylation is required for normal
856 development of linear elements and wild-type meiotic recombination in
857 *Schizosaccharomyces pombe*. Chromosoma 119:59–72. doi: 10.1007/s00412-009-0241-
858 5

859 Stanzione M, Baumann M, Papanikos F, et al (2016) Meiotic DNA break formation requires
860 the unsynapsed chromosome axis-binding protein IHO1 (CCDC36) in mice. Nat Cell Biol
861 18:1208–1220. doi: 10.1038/ncb3417

862 Sung P (1997) Yeast Rad55 and Rad57 proteins form a heterodimer that functions with
863 replication protein A to promote DNA strand exchange by Rad51 recombinase. Genes
864 Dev 11:1111–21.

865 Tripathi P, Pal D, Muniyappa K (2007) *Saccharomyces cerevisiae* Hop1 protein zinc finger
866 motif binds to the Holliday junction and distorts the DNA structure: implications for
867 Holliday junction migration. Biochemistry 46:12530–42. doi: 10.1021/bi701078v

868 Tsubouchi H, Roeder GS (2006) Budding yeast Hed1 down-regulates the mitotic
869 recombination machinery when meiotic recombination is impaired. Genes Dev
870 20:1766–75. doi: 10.1101/gad.1422506

871 Tsutsui Y, Khasanov FK, Shinagawa H, et al (2001) Multiple interactions among the
872 components of the recombinational DNA repair system in *Schizosaccharomyces pombe*.
873 Genetics 159:91–105.

874 Vitelli F, Piccini M, Caroli F, et al (1999) Identification and characterization of a highly
875 conserved protein absent in the Alport syndrome (A), mental retardation (M), midface
876 hypoplasia (M), and elliptocytosis (E) contiguous gene deletion syndrome (AMME).
877 Genomics 55:335–40. doi: 10.1006/geno.1998.5666

878 Woltering D, Baumgartner B, Bagchi S, et al (2000) Meiotic segregation, synapsis, and
879 recombination checkpoint functions require physical interaction between the

880 chromosomal proteins Red1p and Hop1p. Mol Cell Biol 20:6646–58.

881 Young JA, Hyppa RW, Smith GR (2004) Conserved and nonconserved proteins for meiotic
882 DNA breakage and repair in yeasts. Genetics 167:593–605. doi:
883 10.1534/genetics.103.023762

884 Zetka MC, Kawasaki I, Strome S, Müller F (1999) Synapsis and chiasma formation in
885 *Caenorhabditis elegans* require HIM-3, a meiotic chromosome core component that
886 functions in chromosome segregation. Genes Dev 13:2258–2270. doi:
887 10.1101/gad.13.17.2258

888